Numerical analysis of flux and loss distributions in electrical machinery (invited)

Takayoshi Nakata
Okayama University

NUMERICAL ANALYSIS OF FLUX AND LOSS DISTRIBUTIONS IN ELECTRICAL MACHINERY (invited)

T.Nakata

ABSTRACT

In recent years, techniques of numerical analysis have rapidly progressed. By introducing these techniques, the design of smaller and more efficient electrical machinery becomes easier without repeating trial manufacture which is time consuming, laborious and money wasteful.

The paper describes the present status of the numerical simulation of flux and loss distributions in electrical machinery, mainly transformers.

1. INTRODUCTION

Loss evaluation has become important because of high energy cost. Therefore, it is necessary to know in detail the behaviour of flux in electrical machinery in order to develop smaller cores with higher efficiency. The quantitative analysis of localized flux and loss distributions has become easier through the remarkable progress of numerical field calculations such as the finite element method [1-5]. The numerical simulation is more effective and economical than experimental method. Moreover, useful suggestions for improving electrical machinery can be obtained from the calculated flux and loss distributions.

In this paper, firstly, the factors which increase iron losses in electrical machinery are discussed. Secondly, the effects of core constructions, joints and hysteresis on flux distributions are examined. Thirdly, the present status of the estimation techniques of iron losses produced by distorted fluxes and rotating fluxes is explained. Lastly, the optimum design of cores using the finite element method is discussed.

2. FACTORS AFFECTING THE BUILDING FACTOR

The measured iron loss of transformer core is usually larger than that simply calculated as the product of the core weight and the specific loss (W/Kg) of core material. The ratio of the above-mentioned two kinds of losses is often called the "building factor". The building factor (B.F.) is defined by the following equation:

$$B.F.=\frac{\text{iron loss of laminated core(W/Kg)}}{\text{iron loss of material measured by SST(W/Kg)}} \quad (1)$$

where SST means the single sheet tester [6].

The causes which increase the iron losses of cores are as follows:

(1) Non-uniform flux distribution due to the difference in path lengths among magnetic circuits,
(2) Distortion of flux waveform due to magnetic saturation,
(3) Circulating flux due to magnetic anisotropy of material,
(4) Flux directed out of the rolling direction,
(5) Rotating flux due to three-phase magnetomotive forces,
(6) Transverse flux between layers due to joints,
(7) Interlaminar short circuits,
(8) Deterioration of magnetic characteristics due to mechanical stress.

Factors (7) and (8) are to be controlled in the manufacturing process. Therefore, the factors from (1) to (6) are investigated in this paper.

The above-mentioned factors are affected by the following items:

(1) Factors which can be controlled by steel manufacturers,
  (a) anisotropy of the magnetizing characteristics,
  (b) shape of the hysteresis curve.
(2) Factors which can be controlled by manufacturers of electrical machinery,
  (a) core geometry,
  (b) joint configuration.

Other factors affecting the building factor are,
  (a) shape of iron loss curve and its anisotropy,
  (b) ratio of hysteresis loss to eddy current loss.

These factors can be controlled by the steel manufacturers.

If a new material which has magnetic characteristics such that the percentage of eddy current loss to the total iron loss is lower and the anisotropy of iron losses is smaller could be developed, the building factor of a core made from such a new material would be reduced [7,8]. As the effects of the other factors are so complicated, further examinations are necessary.

3. EFFECTS OF CORE CONSTRUCTIONS

Localized flux distributions in various types of cores have been analyzed. Figure 1 shows the flux distributions in core-type three-phase three-limbed transformer cores [1,2,8]. Figures 1(a) and (b) show the influence of the core material on the flux distributions. The maximum flux density "Bleg" in the limb is equal to 1.7(T). The core in Fig. 1(a) is made of 0.35(mm) thick conventional grain-oriented silicon steel M-5 and that in Fig.1(b) is made of 0.3(mm) thick highly-oriented silicon steel M-OH. Some flux penetrates into the middle limb at $\omega t=90°$ and into the right-side limb at $\omega t=30°$. The flux is called the "circulating flux". The circulating flux is increased in the high quality core due to the higher anisotropy.

Figures 1(c) and (d) show the effect of the window height on flux distributions. The percentage of the volume of the yoke in Fig.1(c), in which the flux does not flow uniformly, is larger than that in Fig.1(d). Therefore, the iron loss (W/kg) of the lower window core in Fig. 1(c) is larger than that of the higher window core in Fig. 1(d).

Figures 1(e) and (f) show the effect of the joint-angle θ in the T-joint on flux distributions. With the increase of θ, the circulating flux in the middle limb at $\omega t=90°$ decreases. As a result, the distortion of flux waveform is improved.

4. EFFECTS OF JOINTS

Effects of joints on the increase of core loss have been analyzed using the newly developed "time periodicity finite element method" [10] and the periodicity condition [11,12].

Figure 2 illustrates the influence of the overall

The author is with the Department of Electrical Engineering, Okayama University, Okayama 700, Japan.

0018-9464/84/0900-1750$01.00©1984 IEEE

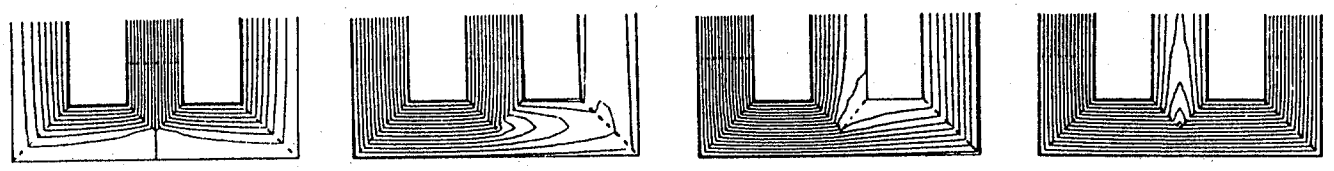

(a) standard size (M-5,0.35mm)

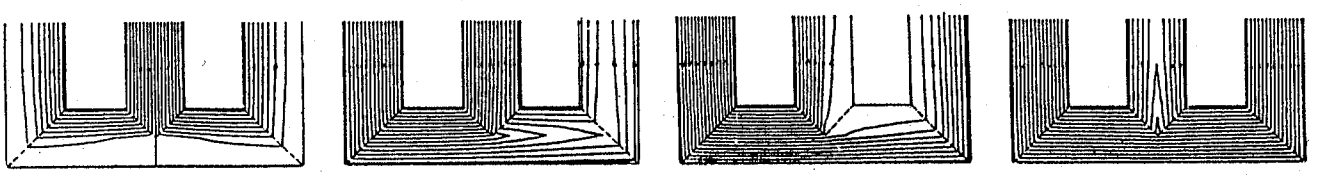

(b) standard size (M-0H,0.3mm)

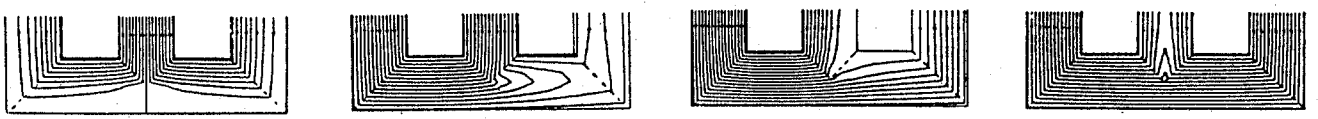

(c) low window size (M-5,0.35mm)

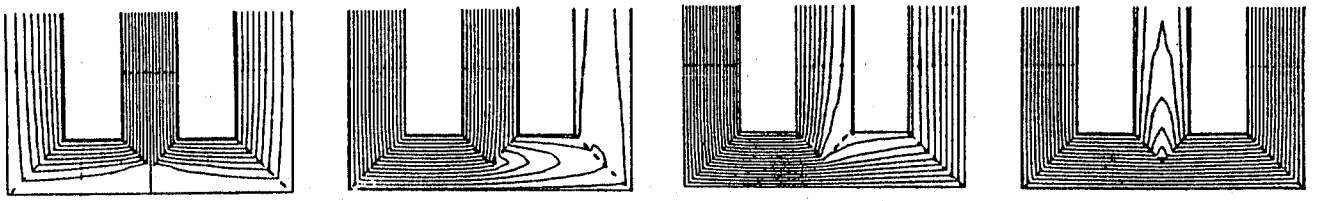

(d) high window size (M-5,0.35mm)

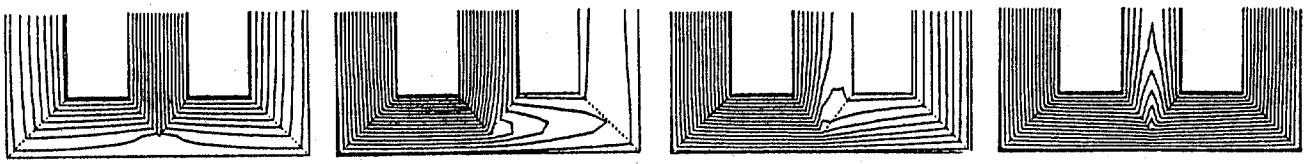

(e) joint of acute angle (θ=74°,M-0H,0.3mm)

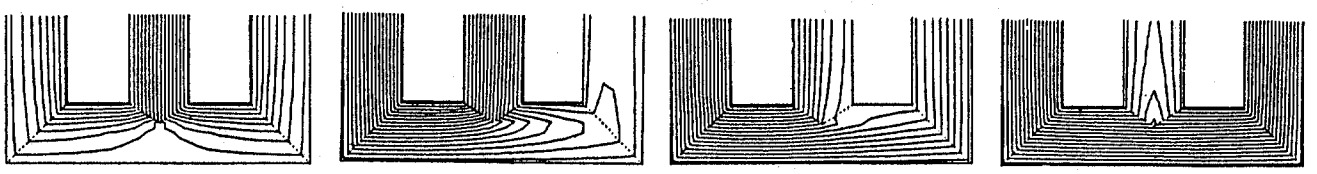

ωt=0° ωt=30° ωt=60° ωt=90°

(f) joint of obtuse angle (θ=113°,M-0H,0.3mm)

Fig. 1 Effects of core construction on flux distributions (Bleg=1.7T).

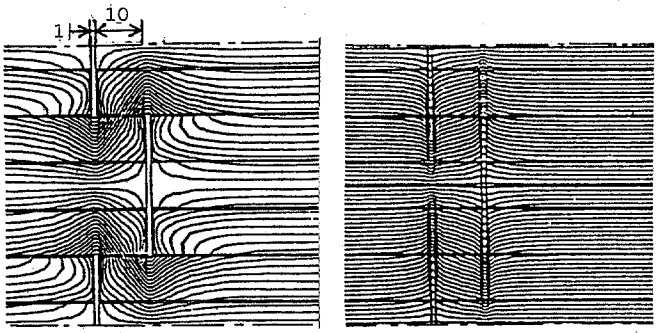

(a) low flux density (Bm=1.0T) **(b) high flux density (Bm=1.7T)**

Fig. 2 Flux distributions near lap joint (M-3H,0.3mm,n=3,50Hz).

flux density Bm on the flux distributions in a straight overlap joint [11]. n denotes the number of laminations per stagger layer. Because of symmetry, only a part of the whole flux distribution is denoted. The dimensions in the y-direction of these figures are expanded 33 times for clarity. The transverse flux in the interlaminar gap concentrates near the joint with the increase of the flux density Bm. The flux passing through the air gap at the joint is increased with Bm. About 30(%) of the total flux passes through the air gap at the usual operating flux density.

Figure 3 shows that the flux distribution when the magnetic field is increasing is very different from that when the magnetic field is decreasing due to eddy current [11].

If the arrangement of the gap at the joint is irregular due to human errors, the iron loss is considerably increased. An example of the flux

distribution for irregular arrangement is shown in Fig. 4. The flux distribution near the irregular gaps is more complicated than that in the regular arrangement shown in Fig. 5. As the iron losses are considerably increased by the small irregularities, special attention should be paid in manufacturing laminated cores with lap joints. This example suggests that the numerical simulation can be applicable to the management of core production.

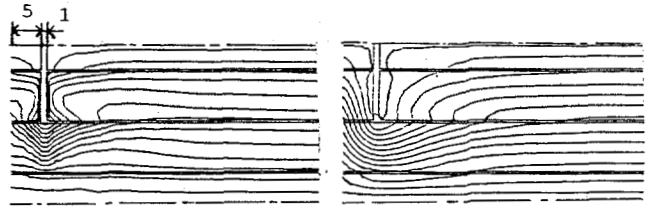

(a) magnetic field is increasing(ωt=45°) (b) magnetic field is decreasing(ωt=135°)

Fig. 3 Effect of eddy current on flux distributions (M-3H,0.3mm,n=3,Bm=1.0T,50Hz).

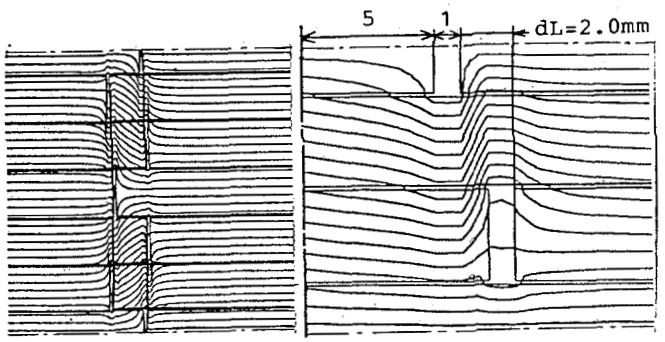

(a) total flux distribution (b) enlarged flux distribution

Fig. 4 Flux distribution for irregular arrangement (M-3H,0.3mm,n=1,Bm=1.7T,50Hz).

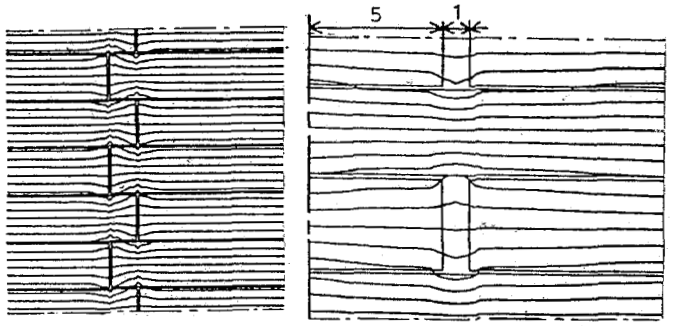

(a) total flux distribution (b) enlarged flux distribution

Fig. 5 Flux distribution for regular arrangement (M-3H,0.3mm,n=1,Bm=1.7T,50Hz).

5. EFFECTS OF HYSTERESIS

Figures 6 and 7 show the influence of the hysteresis characteristics on the flux distributions of a single-phase two-limbed transformer core. If the hysteresis characteristics are neglected, the flux vanishes at ωt=90° as shown in Fig. 6(c). However, if the hysteresis characteristics are taken into account, circulating fluxes exist at ωt=90°as shown in Fig. 7(c). The difference between the flux distributions at ωt=75°and 105° is also caused by the hysteresis effect.

Figure 8 shows the waveforms of the localized flux densities. The waveform of each localized flux density is non-symmetrical. The difference in phase angles among the localized flux densities is caused by the hysteresis effect. When the grade of the silicon steel goes up, the distortion of the flux waveform is decreased. In the case of a three-phase transformer core, the phase shift is decreased compared with the case of the single-phase core.

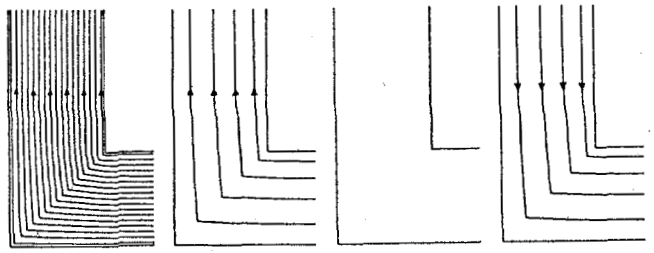

(a) ωt=0° (b) ωt=75° (c) ωt=90° (d) ωt=105°

Fig. 6 Flux distributions without hysteresis (M-4,0.3mm,Bleg=1.7T).

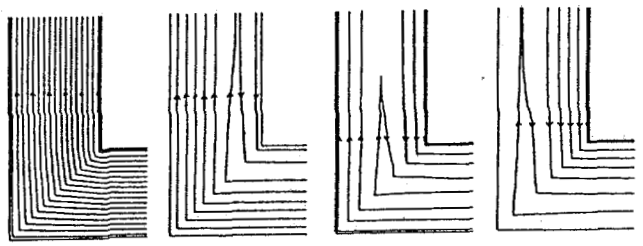

(a) ωt=0° (b) ωt=75° (c) ωt=90° (d) ωt=105°

Fig. 7 Flux distributions with hysteresis (M-4,0.3mm,Bleg=1.7T).

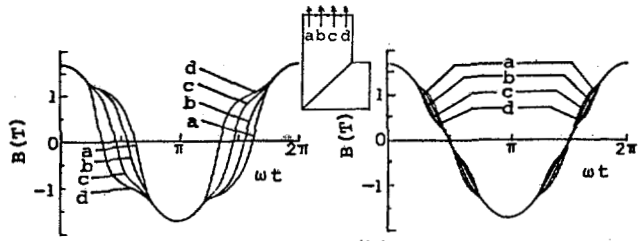

(a) with hysteresis (b) without hysteresis

Fig. 8 Waveforms of localized flux densities (M-4,0.3mm,Bleg=1.7T).

6. ESTIMATION OF IRON LOSSES

A reliable method for estimating iron losses should be established in order to analyze the iron loss distribution from the flux distribution obtained numerically.

6.1 Iron Losses due to Distorted Fluxes

Figure 9 shows an example of the flux density waveforms in a three-phase three-limbed transformer core excited by a sinusoidal voltage source. In general, the flux in each part of the core is distorted due to the magnetic saturation, the difference in magnetic path lengths and the anisotropy of the material as mentioned in the previous sections.

Let us assume that the instantaneous flux density b is given by,

$$b = B_1 \sin \omega t + \Sigma B_n \sin n(\omega t + \theta_n) \qquad (2)$$

where B_1 and B_n are the amplitudes of the fundamental and the n-th harmonic component respectively, and θ_n is the phase angle of the n-th harmonic component. Σ

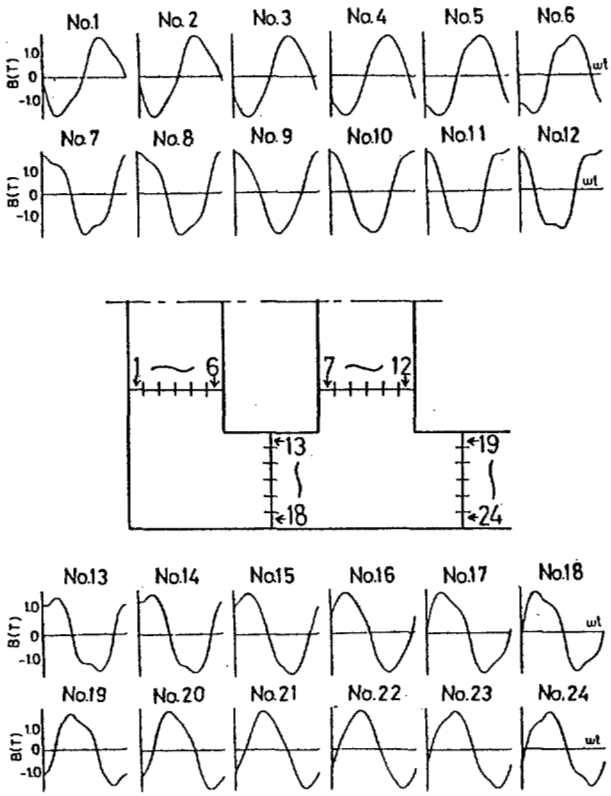

Fig. 9 Waveforms of localized flux densities in a three-phase three-limbed core (measured,M-5,0.35mm,Bleg=1.7T).

represents the summation for all components.

The iron loss due to the distorted flux can be estimated by the following equations [13,14].

$$W = W_h + W_e \tag{3}$$

$$W_h = \omega_h(B_m) + 2\sum_{i=1}^{m} \omega_h(B_{ki}) \tag{4}$$

$$We = K \cdot \omega_e(B_e) \tag{5}$$

where

Wh: hysteresis loss (W/Kg)
We: eddy current loss (W/Kg)
$\omega_h(B_m)$: function of hysteresis loss
$\omega_e(B_e)$: function of eddy current loss

Be is the maximum flux density of the sinusoidal wave which gives the same effective voltage as that of the distorted flux. Hence, Be is defined by the following equation.

$$B_e = \sqrt{\Sigma (nB_n)^2} = F \cdot Bm \tag{6}$$

Where

$$F = \frac{2\sqrt{2}}{\pi} FF \tag{7}$$

FF is the form factor. Bki is the amplitude of the minor loop and m is the number of the groups of minor loops. Σ represents the summation of losses caused by the minor loops which appear in a half cycle successively. The functions ω_h and ω_e may be determined by the method for separating the hysteresis loss and the eddy current loss developed by us [13]. K is a calibration factor which is a function of Bm and θn. The values Bm, Be and Bki can be easily obtained from the numerical calculation.

When the flux flows in the rolling direction and the minor loops are small enough, the accuracy of Eq.(3) is within ±5(%) in the region of the flux density in practical use. Figures 10(a) and (b) show the errors ε of the predicted iron losses of

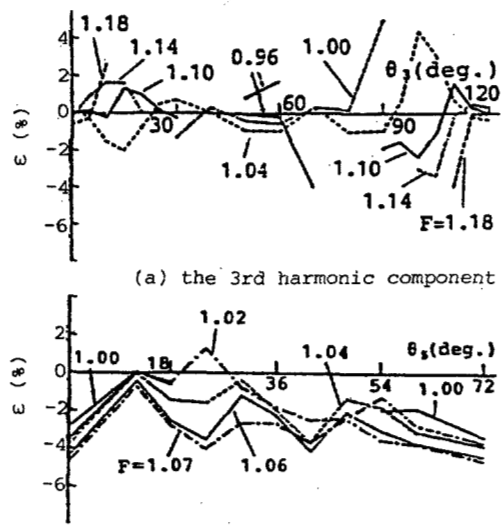

(a) the 3rd harmonic component

(b) the 5th harmonic component

Fig. 10 Errors of predicted iron losses (M-5,0.35mm,Bleg=1.7T,50Hz).

grain-oriented silicon steel M-5 produced by the distorted fluxes containing the 3rd and the 5th harmonic components respectively.

When the flux does not flow in the rolling direction, the iron losses are usually estimated by the following equation [7].

$$W = W_R + W_T \tag{8}$$

Where, W_R and W_T denote the iron losses in the rolling and the transverse directions respectively. These are calculated from Eq.(3) by using the loss curves in the rolling and the transverse directions respectively. In this case, the flux densities Bm and Be in Eqs.(4), (5) and (6) are those in the rolling and the transverse directions respectively. Equation (8) should be more closely examined in order to establish the accurate estimation of iron losses in all directions. When the distorted flux contains large minor loops, the above-mentioned equations cannot be used [14].

6.2 Iron Losses due to Rotating Fluxes

Figure 11 shows the loci of the flux density in the stator of a synchronous machine. Although, near the core back, the flux is apparently alternating in the circumferential direction of the stator, the loci of the flux densities behind the teeth are circular. In the teeth, the vector is alternating and directed

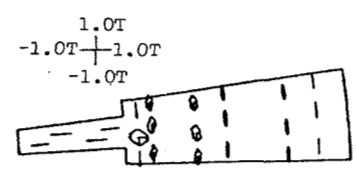

(a) non-oriented core (M-15,0.35mm)

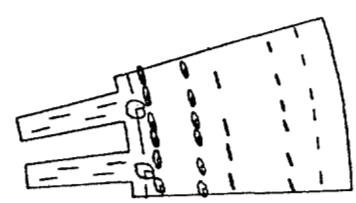

(b) oriented core (M-5,0.35mm)

Fig. 11 Loci of flux density vectors in stator cores.

radially. Rotating fluxes also exist in the so-called T-joints of three-phase transformer cores due to three-phase magnetomotive forces.

The rotating flux causes a large additional iron loss. The iron loss due to rotating flux without any harmonic component can be estimated from the lengths of the major and the minor axes, and the angle between the direction of the major axis and the rolling direction [15]. When the rotating flux is distorted, the estimation of the iron loss is extremely difficult because the amplitude and the phase angle of the harmonic flux affect the iron loss. The establishment of a method for estimating the iron loss due to distorted rotating flux is desired.

A new technique is being proposed [16]. The numerical calculation of the flux distribution is combined with a microprocessor controlled magnetic tester which would interactively measure the rotational loss in single samples under the same field conditions solved for the model and the experimental data would be inputted to the main computer to accurately obtain the localized loss distribution.

It is very important to discuss the distribution of iron losses. However, the present status of estimation techniques is not sufficient for the discussion of the building factor.

7. OPTIMUM DESIGN

Here, the optimum design means to design an efficient, small and high performance machinery with low loss, low volume, low noise etc. The core losses can be minimized by controlling adequately the flux distributions and the flux waveforms. The noises due to the electromagnetic forces of the core can also be reduced by adjusting the shape of the core so that the flux distribution may become uniform. Therefore, the flux should be controlled so that the optimum electrical machinery may be designed. There are two kinds of control methods. One is the control of the magnetization curves, which is carried out by the steel manufacturers. The other is the control of the positions, the sizes and the shapes of cores, which is carried out by the manufacturers of electrical machinery.

Two examples of controlling fluxes are shown in this section. These are analyzed using the "finite element method for inverse problems" [17-19]. In the conventional finite element method, the flux distribution in the core made from the given material and of the given shape is analyzed. On the contrary, in the finite element method for inverse problems, the magnetic characteristics of the material and the shape of the core which satisfy the prescribed flux distribution can be calculated [17-19].

7.1 Optimum magnetization curves

The method for determining the optimum magnetization curves of the material used is discussed under the condition that the shape of the core is fixed. The flux can also be controlled by inserting some materials such as equivalent air gaps in series or in parallel with the magnetic paths instead of changing the magnetization curve.

Figure 12 shows an example of the control of flux distributions [20]. Figure 12(a) shows the waveforms of flux density at joint of a single-phase two-limbed transformer core. The waveform in each part is distorted, and the maximum value of the waveform B_1 near the window is larger than that of B_6 in the outer side. This is caused by magnetic saturation and the difference between magnetic path lengths. Figure 12(b) denotes the waveforms of flux density in a core in which the flux waveforms are controlled using the above-mentioned method so that the maximum value of each waveform can be the same. Figure 12(c) shows the other controlled waveforms. In this case, the waveforms are controlled so that the waveform in every part can be approximately the same. The waveforms obtained are nearly sinusoidal.

In conventional research, steel manufacturers and manufacturers of electrical machinery have independently investigated the optimum magnetic characteristics of silicon steel and the optimum construction of iron core respectively by trial and error. Therefore, it was impossible to examine the optimum iron core from the synthetic point of view. Now, the manufacturers of electrical machinery have reached the stage to specify the steel manufacturers to produce the silicon steel with the most preferable magnetic characteristics for respective iron cores from the point of view of the optimum design. The co-investigation of steel manufacturers and manufacturers of electrical machinery is hoped in order to develop the most suitable magnetic material for cores.

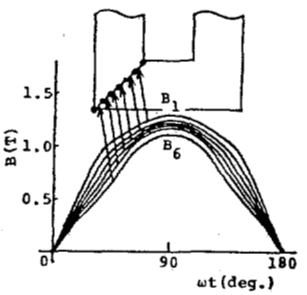

(a) without special control

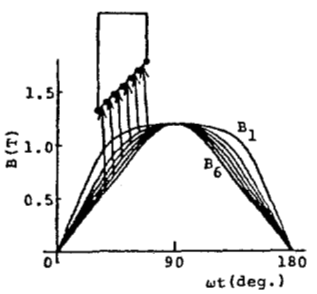

(b) with special control so that the maximum values may be the same

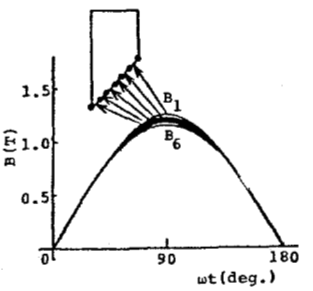

(c) with special control so that the distortions may be reduced

Fig. 12 waveforms of flux densities at the joint (M-OH,0.3mm,Bleg=1.7T).

7.2 Optimum positions

The method for determining the optimum positions of core blocks for a power reactor is discussed under the condition that the quality of core material is given.

Figure 13(a) denotes the flux distribution of a conventional power reactor. The low-noise reactor the attractive forces of which is the minimum is obtained by changing the position of each core block so that the fluxes on the upper and the lower sides of each core block may become uniform. In this calculation, the total gap length is also adjusted so that the inductance of the obtained reactor may be the same as that of Fig. 13(a). The flux distribution of the obtained low-noise reactor is shown in Fig. 13(b).

It is also possible to determine the sizes and the shapes of cores using this method.

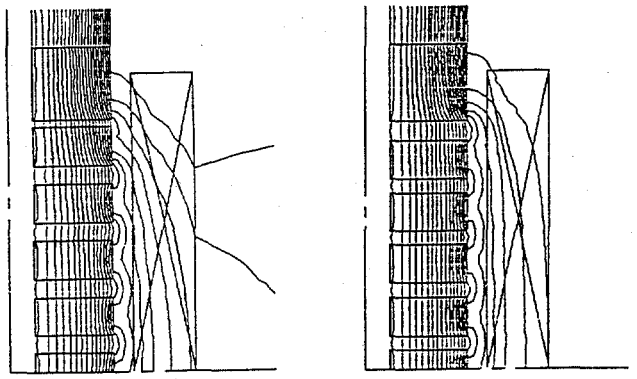

(a) conventional type (b) low-noise type

Fig. 13 Flux distributions of reactors (M-5,0.35mm).

8. CONCLUSIONS

The present status of the numerical simulation of flux and loss distributions in electrical machinery is discussed. The optimum design of electrical machinery using the finite element method is also explained.

Although only several examples are discussed in this paper, it is possible to analyze many kinds of machinery under various conditions using, for example, the following techniques:

(1) Finite element method for analyzing under given voltage [17]:

Flux distributions on load can be analyzed from the applied voltage instead of the exciting current which is usually unknown when the electrical machinery is connected with the constant voltage source.

(2) Efficient technique using special elements such as gap element [21], shielding element and so on:

The investigation of the effects of positions and widths of gaps or shields on the magnetic characteristics of electrical machinery is laborious using the usual finite element method because it needs re-subdivision. If the gap elements or the shielding elements are used, it becomes easy to investigate the effects.

As the localized flux in electrical machinery is distorted, new materials with low eddy current losses such as thinner sheet and scratched sheet[22] should be developed. The most suitable magnetizing curve for the core of electrical machinery may exist because the flux distributions are affected by the shape of the magnetization curve. The co-investigation of manufacturers of electrical machinery and steel manufacturers is hoped in order to develop the most suitable magnetic material for cores.

Further work will help manufacturers of electrical machinery to optimize their design.

REFERENCES

[1] T. Nakata, "Analysis of Flux Distribution of Three-Phase, Three-Limbed Transformer Cores", Electrical Engineering in Japan, 95, 3, 43 (1975).

[2] T. Nakata, Y. Ishihara, K. Yamada and A. Sasano, "Non-Linear Analysis of Rotating Flux in the T-Joint of a Three-Phase, Three-Limbed Transformer Core", European Physical Society Conference, Proceedings of Soft Magnetic Materials 2, 4-5, 57 (1975).

[3] T. Nakata, Y. Ishihara and N. Takahashi, "Numerical Solution of Flux Distributions in Transformer Cores", International Symposium on Electrodynamics, Forces and Losses in Transformers, C2, 243 (1979).

[4] T. Nakata, "Recent Research in Numerical Analysis of Transformer Cores", CIGRE Study Committee No. 12 Colloquium (1983).

[5] A. Basak and C. R. G. Higgs, "Flux Distribution in Three Phase Transformer Cores with Various T-Joint Geometries", IEEE Trans. on Magnetics, MAG-18, 2, 670 (1982).

[6] T.Nakata, Y. Ishihara, N. Takahashi and Y. Kawase, "Analysis of Magnetic Fields in a Single Sheet Tester Using an H Coil", Journal of Magnetism and Magnetic Materials, 26, 1-3, 179 (1982).

[7] M. Okabe, M. Okada and H. Tsuchiya, "Effects of Magnetic Characteristics of Materials on the Iron Loss in the Three Phase Transformer Core", IEEE Trans. on Magnetics, MAG-19, 5, 2192 (1983).

[8] T. Nakata and N. Takahashi, "Finite Element Analysis of Transformer Cores", Memoirs of the School of Engineering, Okayama University, 18, 1 (1984).

[9] T. Nakata and N. Takahashi, "The Finite Element Method in Electrical Engineering", Tokyo, Morikita Publishing Co. Ltd.. (1982) (book).

[10] T. Nakata, Y. Kawase, M. Matsubara and S. Ito, "Analysis of Characteristics of Electromagnets with Shading Coil Using the Time Periodicity Finite Element Method", Trans. of IEE Japan (1984) (to be published).

[11] T. Nakata and Y. Kawase, "Finite Element Analysis of Magnetic Characteristics in Straight Overlap Joints of Laminated Cores", ibid., 103-B, 5, 357 (1983).

[12] T. Nakata and Y. Kawase, "Analysis of Magnetic Characteristics in Straight Overlap Joints of Laminated Cores", Electrical Engineering in Japan, 102, 1, 78 (1982).

[13] T. Nakata and Y. Ishihara and M. Nakano, "Iron Losses of Silicon Steel Core Produced by Distorted Flux", ibid., 90, 1, 10 (1970).

[14] T. Nakata, Y. Ishihara and M. Nakano, "Experimental Studies of Various Factors Affecting Minor Loop Hysteresis Loss", Memoirs of the School of Engineering, Okayama University, 8, 1, 1 (1973).

[15] Y. Ishihara and N. Takahashi, "Iron Losses of Silicon Steel due to Rotating Fluxes", ibid., 14, 1, 15 (1979).

[16] A. J. Moses, "Factors Affecting Localised Flux and Iron Loss Distribution in Laminatd Cores", Journal of Magnetism and Magnetic Materials, 41, 1-3 (1984).

[17] T. Nakata and N. Takahashi, "Direct Finite Element Analysis of Flux and Current Distributions under Specified Conditions", IEEE Trans. on Magnetics, MAG-18, 2, 325 (1982).

[18] T. Nakata and N. Takahashi, "Application of the Finite Element Method to the Design of Permanent Magnets", ibid., MAG-18, 5, 1049 (1982).

[19] T. Nakata and N. Takahashi, "New Design Method of Permanent Magnets by Using the Finite Element Method", ibid., MAG-19, 6, 1494 (1983).

[20] T. Nakata, N. Takahashi, Y. Kawase and K. Fujiwara, "Control of Flux Distributions in Transformer Cores", Journal of Magnetism and Magnetic Materials, 41, 1-3 (1984).

[21] T. Nakata, Y. Ishihara and N. Takahashi, "Finite Element Analysis of Magnetic Fields by Using Gap Element", Proceedings of Compumag Conference, 5-7 (1978).

[22] I. Ichijima, M. Nakamura, T. Nozawa and T. Nakata, "Improvement of Magnetic Properties in Thinner HI-B with Domain-Refinement," IEEE Trans. on Magnetics, MAG-20, 5 (1984).